

BeFA: A General Behavior-driven Feature Adapter for Multimedia Recommendation

Qile Fan*
Nanjing University of Posts and
Telecommunications
Nanjing, China
b21011331@njupt.edu.cn

Penghang Yu*
Nanjing University of Posts and
Telecommunications
Nanjing, China
2022010201@njupt.edu.cn

Zhiyi Tan
Nanjing University of Posts and
Telecommunications
Nanjing, China
tzy@njupt.edu.cn

Bing-Kun Bao
Nanjing University of Posts and
Telecommunications
Nanjing, China
bingkunbao@njupt.edu.cn

Guanming Lu†
Nanjing University of Posts and
Telecommunications
Nanjing, China
lugm@njupt.edu.cn

ABSTRACT

Multimedia recommender systems focus on utilizing behavioral information and content information to model user preferences. Typically, it employs pre-trained feature encoders to extract content features, then fuses them with behavioral features. However, pre-trained feature encoders often extract features from the entire content simultaneously, including excessive preference-irrelevant details. We speculate that it may result in the extracted features not containing sufficient features to accurately reflect user preferences.

To verify our hypothesis, we introduce an attribution analysis method for visually and intuitively analyzing the content features. The results indicate that certain products' content features exhibit the issues of **information drift** and **information omission**, reducing the expressive ability of features. Building upon this finding, we propose an effective and efficient general **Behavior-driven Feature Adapter (BeFA)** to tackle these issues. This adapter reconstructs the content feature with the guidance of behavioral information, enabling content features accurately reflecting user preferences. Extensive experiments demonstrate the effectiveness of the adapter across all multimedia recommendation methods. The code will be publicly available upon the paper's acceptance.

KEYWORDS

Multimodal Recommendation, Feature Adapter, Information Drift, Information Omission

1 INTRODUCTION

Recommender systems have gained widespread adoption across various domains, aiming to assist users in discovering information that aligns with their preferences [17, 22]. In the case of multimedia platforms, the abundance of data resources provides recommender systems with increased opportunities to accurately model user preferences [47].

Existing multimedia recommendation methods typically involves two main steps [41, 47]. First, a pre-trained feature encoder is employed to capture content features from diverse modalities. Subsequently, these content features are fused with behavioral features

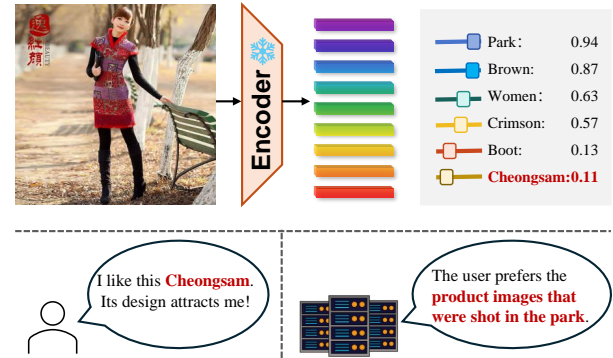


Figure 1: Illustration of content features that do not accurately reflect the users' preferences. Excessive irrelevant information hinders the recommender system's ability to effectively model the users' true preferences.

to obtain user preference representations. Recently, researchers have focused on enhancing the quality of these representations through self-supervised learning. For instance, SLMRec [29] investigates potential relationships between modalities through the use of contrastive learning, thereby obtaining a powerful representation. BM3 [52] utilizes a dropout strategy to construct multiple views and reconstructs the interaction graph, incorporating intra- and inter-modality contrastive loss to facilitate effective representation learning. MICRO [43] and MGCN [40] maximize the mutual information between content features and behavioral features with a self-supervised auxiliary task, and have achieved excellent performance.

Despite the good progress made by existing methods in utilizing content and behavioral information more effectively, a crucial yet easily overlooked problem arises: **Are content features obtained from pre-trained encoders containing sufficient features to reflect user preferences?** Intuitively, multimedia content inherently exhibits the characteristic of low informational value density, where a significant portion of the presented information may be irrelevant to the users' focus [43, 47]. Pre-trained feature encoders extract information from the entire content simultaneously, which

*Both authors contributed equally to this research.

†Corresponding authors



Figure 2: Results of visualisation attribution analysis on the TMALL dataset.(a) is the original product image and (b) is its corresponding heatmap.

can result in content features that do not truly reflect the users’ preferences (as shown in Figure 1). Fusing these irrelevant content features with behavioral features may mislead user preference modeling, resulting in suboptimal recommendation performance.

To answer this question, we introduce a similarity-based attribution analysis method for visualizing and intuitively analyzing the content features. This method evaluates the extent to which content features can reflect user preferences, enabling researchers to visually assess the quality of content features for the first time. The results indicate that not all products’ content features accurately reflect user preferences. Due to the presence of irrelevant information, certain products’ content features exhibit the issues of **information drift** and **information omission**. As shown in Figure 2, some products’ content features do not include information about the products that users are interested in, but instead erroneously include information about unrelated items, a phenomenon we term **information drift**. There are also some products’ content features that omit certain key details of the products, which we refer to as **information omission**. These issues ultimately prevent recommender systems from accurately modeling user preferences. To verify the rationality of these findings, we provide a theoretical analysis and explanation. Furthermore, we propose a plug-and-play general **Behavior-driven Feature Adapter (BeFA)** to address the discovered issues. This adapter effectively decouples, filters and reconstructs content features, leveraging behavioral information as a guide to obtain more precise representations of content information. Extensive experiments demonstrate the adapter’s effectiveness across various multimedia recommendation methods and feature encoders.

Our main contributions can be summarized as follows:

- We introduce a similarity-based visual attribution method, which enables researchers to visually analyze the quality of content features for the first time.
- We experimentally revealed the issues of information drift and information omission in content features. We also provide a theoretical analysis to validate the rationality of these findings.
- We propose a general behavior-driven feature adapter, which obtain more precise content representation through decoupling and reconstructing content features.

2 RELATED WORKS

2.1 Multimedia Recommendation

Collaborative filtering (CF)-based approaches have achieved great success in recommender systems, relying on behavioral similarities to make top-k recommendations [21, 44]. Since user preferences are usually influenced by multimodal information, it facilitates researchers to integrate multimodal content information into CF-based approaches with the aim of improvement. Typically, content features are first extracted using pre-trained neural networks and then fused with behavioral features to enhance preference modeling [6, 41]. Considering that behavioral information can be naturally modeled as a bipartite graph structure, researchers begin work on recommender systems based on Graph Convolutional Network(GCN) [1, 38]. For instance, MMGCN [42] constructs modality-specific user-item interaction graphs to model user preferences specific to each modality. LATTICE [42] adds links between items with similar modality characteristics and create a separate item-item graph for each modality. FREEDOM [51] constructs item-item graphs to help learn item semantic relations and reduces the graphs according to the sensitivity edge pruning technique. Meanwhile, researchers began to focus on enhancing the quality of representations through self-supervised learning. BM3 [52] learns user and item representations by reconstructing the user-item interaction graph and aligning modality features from both inter and intra-modality perspectives. MGCN [40] comprehensively models user preferences by adaptively learning the relative importance of different modality features.

However, existing methods usually directly utilize features extracted from pre-trained feature encoders as side information for each item. The pre-trained feature encoders are trained on large-scale datasets collected from the natural world. The features of natural data and e-commerce data are very different. In e-commerce scenarios, the content information often contains a lot of irrelevant information and exhibits the characteristic of low value density. For example, only a small portion of the content image contain relevant information, while the rest is considered noise. This disparity leads to a substantial amount of noise in the content features extracted by pre-trained encoders when applied to multimodal recommender systems. Consequently, the content features do not contain enough

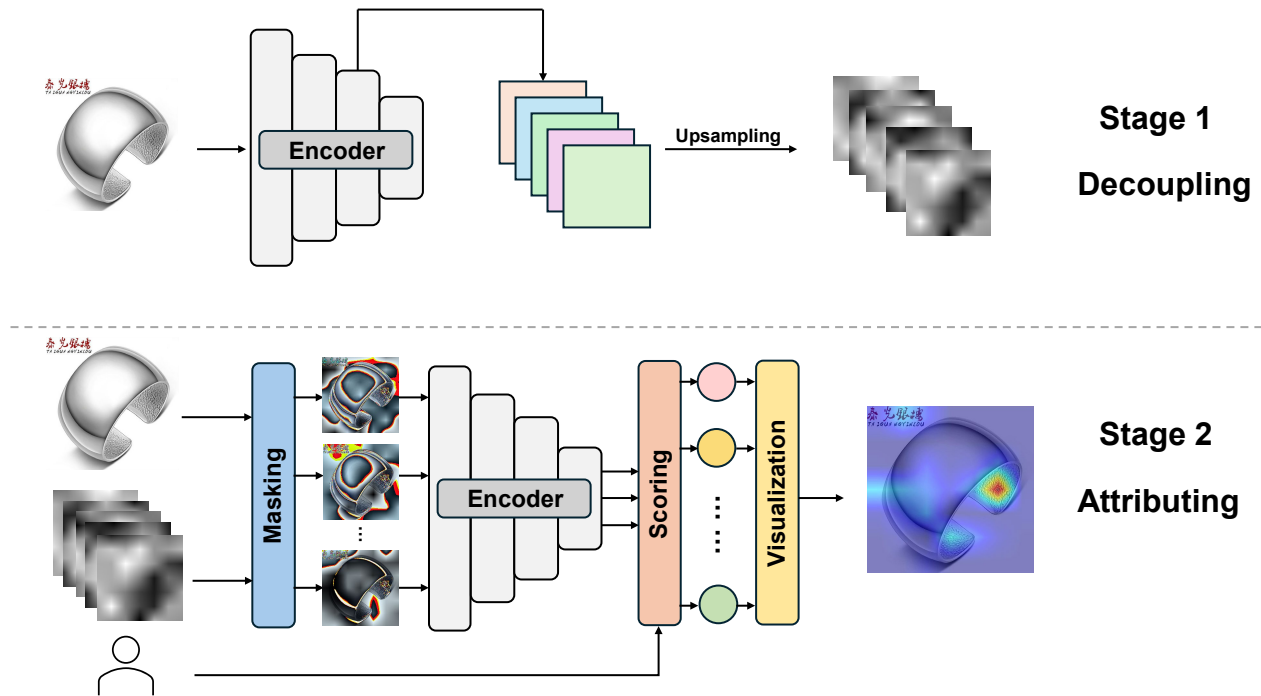


Figure 3: Pipeline of the proposed attribution analysis method.

features to sufficiently reflect users’ preferences. Fusing these irrelevant content features with behavioral features may mislead user preference modeling, resulting in suboptimal recommendation performance.

2.2 Attribution Analysis

Methods for modality feature attribution analysis have been widely studied, aiding in the visualization of modality feature content. Class Activation Mapping (CAM) [46] is a method used to visualize the decision-making process of convolutional neural networks by generating heatmaps that highlight regions of an image contributing to a particular class prediction. Grad-CAM [27] enhances this by using the gradient of the target class with respect to the feature maps of a specific convolutional layer, creating heatmaps that can be applied to various network architectures without altering the network structure. Score-CAM [33] further improves upon Grad-CAM by weighting the activation map using output scores instead of gradient information, thus avoiding gradient-related problems. In multimodal recommender systems, t-SNE [31] is often used to visualize the distribution of samples in high-dimensional feature spaces, providing insights into the relationships and distributions among different modality features.

However, current methods [2, 10] for analyzing image feature weights predominantly rely on CAM-based methods. The heatmaps generated by these methods only reflect the contribution of certain image regions to classification tasks or the relevance of text features, failing to capture the role of multimodal features in recommender systems. Most existing multimodal recommendation

works use t-SNE [31] to analyze the modality features because t-SNE can visualize multimodal feature distributions. But t-SNE can only show the distribution of features in 2-dimensional space, which lacks the intuitive effectiveness of CAM-generated heatmaps and is not suitable for understanding and analyzing specific content features. Consequently, existing attribution analysis methods exhibit significant deficiencies in analyzing multimodal features within multimodal recommender systems.

2.3 Parameter-Efficient Adaptation

In the field of computer vision (CV) and natural language processing (NLP), several studies have identified that semantic differences can restrict the expressiveness of features, thereby impacting the model’s performance as well as downstream tasks [12, 26]. To address this challenge, researchers have explored techniques such as fine-tuning and adapters to bridge these semantic differences [7, 8, 13]. However, in the context of recommendation scenarios where data is continuously changing and expanding, performing full fine-tuning of the encoder poses significant challenges. It often requires a significant amount of time and computational resources, and it may even lead to a decline in the model’s ability to generalize to new data. Given these practical limitations, retraining the feature encoder from scratch for every change in the data is unrealistic. Most of the existing multimodal recommendation methods directly use pre-trained features without fine-tuning, but the content feature extracted by the pre-trained feature encoders may not be sufficient to reflect the users’ preferences, so we consider introducing feature adapters. One such approach is Low-Rank Adaptation(LoRA) [8],

which reduces the number of trainable parameters by integrating trainable low-rank decomposition matrices into the Transformer architecture. Another approach is Prompt Tuning [13], which offers a different perspective by incorporating learnable embedding vectors, acting as hints, into the inputs of the pre-trained model.

However, adding adapters to the middle layer of the pre-trained model may lead to some information loss. Existing parameter tuning methods are not generalized for recommendation tasks, as they fail to adequately incorporate behavioral information, which intuitively reflects the users’ preferences and is crucial for an effective recommender systems.

3 PRELIMINARIES

In this section, we analyze and prove in detail the problems of the content features extracted by pre-trained encoders for recommendation tasks. In section 3.1 we introduce an attribution analysis for visual attribution analysis of content features in multimodal recommender systems. In section 3.2, we specifically analyze the deficiencies of pre-trained feature encoders. In section 3.3 we analyze and prove the problems from a mathematical and theoretical point of view.

3.1 Attribution Analysis

Existing methods for analyzing the weights of image features are predominantly based on class activation mapping (CAM) [46]. However, the heatmaps generated by CAM only reflect the contribution of certain image regions to the classification task and fail to assess their impact on recommendation models [2, 33]. These limitations restrict our in-depth understanding of modality feature processing in recommender systems. Thus we designed the attribution analysis method for analyzing image features in multimodal recommendations based on the characteristics of recommender systems.

To visually illustrate the issues raised, we introduce a intuitively analysis for the attribution of multimodal features in the recommender system. This method aims to explore the effectiveness of content features extracted by pre-trained multimodal feature encoders in multimodal recommender systems. It also provides a visual demonstration of the effectiveness of our proposed adapter in bridging the gap between the content features extracted by the pre-trained encoders and the features required by the recommender system. To accurately identify which parts of the content features users pay attention to, we use cosine similarity as a measurement. By calculating the cosine similarity of each pixel to the behavioral features in the recommendation models, we generate a saliency heatmap. This heatmap is created by weighting and summing the masked feature maps based on the calculated similarities. This approach visualizes the portions of the content features that are truly effective in the recommendation task, providing a deeper understanding of the role of multimodal features in recommender systems.

$$\text{similarity}(x, y) = \frac{v_x \cdot v_y}{\|v_x\| \cdot \|v_y\|} \quad (1)$$

Similar to the concept behind CAM-based approaches, we choose the target layer for visualization to ensure interpretability [2, 33]. In the case of image encoders, for both ResNet [5] and ViT [3] versions, we select the channels closest to the CLIP prediction

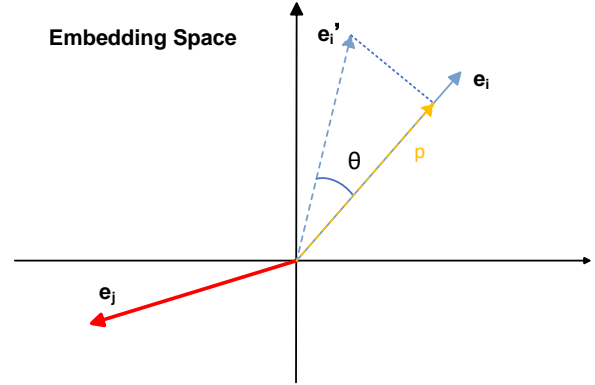


Figure 4: An illustration of a theoretical analysis of deficiency analysis

layer. In convolutional neural networks (CNNs), as the layers go deeper, the information represented in the feature maps becomes more abstract and high-level. The feature maps of the last ReLU layer capture the most important high-level features in the input image. ReLU-activated feature maps contain only positive or zero activations, which helps to emphasize the regions that the model considers more relevant. For the ViT series, as the gradients are zero for all layers except for the [CLS] token and only the [CLS] token is used for final predictions in the last layer embedding, we choose the penultimate layer. Consequently for the ResNet series, we select the last ReLU layer of the final Bottleneck as the target layer, for the ViT series, we use the second-to-last ResidualAttentionBlock as the target layer.

In the first stage, we perform a forward pass of the product images through CLIP, obtaining N channels at the target layer denoted as A_i^N . The purpose is to discriminate the contributions of different targets across different channels. Subsequently, for each channel, we upsample it, denoted as A_i^{up} . This is done to generate masked images corresponding to different parts and to calculate the similarity weights of different regions. In the second stage, element-wise multiplication is performed between each mask A_i^{up} and all color channels x of the input image, and then the result is compared with the corresponding to behavioral features to compute the similarity. We name our method Behavior Information CAM (BeCAM) and its saliency map is computed by:

$$M_{\text{BeCAM}}^i = \sum_i^N A_i \times \text{similarity}((x \odot A_i^{up}), ID_i) \quad (2)$$

where \odot is the Hadamard product.

3.2 Deficiency Analysis

By analyzing the generated heatmap (shown in Figure 2), it is clear that the pre-trained feature encoder suffers from the issues of wrong region of interest and insufficient region of interest on the product dataset. This can be visualized by the fact that the content features extracted by the pre-trained feature encoders have the problems of **information drift** and **information omission**. This is a very visible demonstration of the low information value density of the

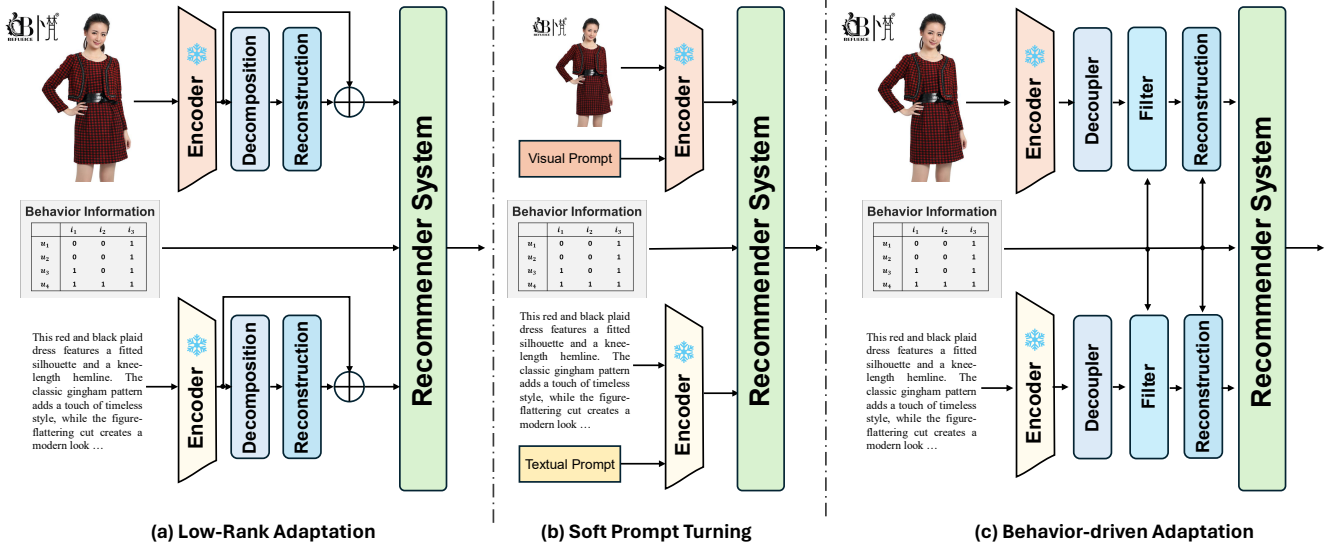


Figure 5: Comparison of efficient parameter tuning methods. (a) Low-Rank Adaptation (b) Soft Prompt Turning (c) Our proposed adapter.

multimedia content itself, resulting the content features are insufficient to reflect users’ preferences.

Specifically, as shown in Figure 2, although the user wants to buy clothes, the feature encoder incorrectly focuses on the model’s face, resulting in **information drift**. There are also products whose content features miss some key details of the product, such as only focusing on certain details of the clothes and failing to focus on its whole, resulting in **information omission**. Information drift can cause the recommender system to ignore useful and critical information. This leads to a loss of important guidance for the recommendation task. It also results in a mismatch between recommendations and users’ preferences. Information omission can result in important visual or textual cues being ignored or incomplete. This causes a loss of critical information needed for the recommendation task. These issues collectively compromise the overall effectiveness of the recommender system. As a result, directly applying the content features extracted by the pre-trained encoder in the multimodal recommender system will inevitably impair the performance of the recommender system.

3.3 Theoretical Analysis

In this section, we reveal the deficiencies of content features extracted by pre-trained feature encoders within the embedding space. We analyze the gap between these content features and the ideal features required by the recommendation model. Furthermore, we demonstrate that optimizing the consistency between the extracted features and the ideal features necessary for accurate recommendation predictions can significantly enhance recommendation performance. This analysis provides theoretical support for the effectiveness of our proposed adapter.

The embedding space captures the semantic relationships and similarities between features. Analyzing features in the embedding

space enables a better understanding and interpretation of their relationships. Formally, considering a node i and its representation e_i in the embedding space, which represents the ideal features required by the recommendation model. On the basis of the item feature representation e_i in the embedding space, the recommender system calculates the probability distribution of the rating or clicking behavior of the user u on the item i , which can be viewed as the prediction $P(r_{ui}|e_u, e_i)$. Where r_{ui} stands for the rating or click behavior of the user u on item i , e_u represents the user’s feature, and e_i signifies the item’s feature. Our objective is to find the optimal user feature e_u and item feature e_i to maximize the posterior distribution $P(r_{ui}|e_u, e_i)$. In other words, we aim to maximize the posterior distribution for the user feature e_u and item feature e_i parameters. This can be formally described by the following objective function:

$$L(e_u, e_i) = \arg \max_{x_u, e_i} P(r_{ui}|e_u, e_i) \quad (3)$$

The representation e'_i extracted by the feature encoder can be seen as the prior distribution. However, due to semantic differences between the natural data and e-commerce data, there is inevitably some deviations between the features extracted by the pre-trained feature encoder and the ideal features. Let us denote this deviation as θ .

$$\theta = \arccos \left(\frac{e_i \cdot e'_i}{\|e_i\| \|e'_i\|} \right) \quad (4)$$

Analyzing θ helps understand the deviation between the features extracted by the feature encoder and the ideal features. A smaller θ indicates that the two representations are very close in the embedding space. This implies a high consistency between the features extracted by the feature encoder and the ideal features, which benefits the recommendation system in accurately capturing user interests and item similarities. By reducing θ , the features become

Table 1: Statistics of the experimental datasets

Dataset	#User	#Item	#Behavior	Density
TMALL	13,104	7,848	151,928	0.148%
Microlens	46,420	14,079	332,730	0.051%
H&M	43,543	16,915	369,945	0.050%

closer to the ideal features, thereby enhancing the performance of the recommendation system.

The part p of the representation e'_i extracted by the encoder that is truly effective for the recommendation task can be represented as follows:

$$p = \left(e'_i \cdot \frac{e_i}{\|e_i\|} \right) \frac{e_i}{\|e_i\|} = e'_i \cdot \cos(\theta) \quad (5)$$

When the deviation θ is large, as e'_i in Figure 4, content features exhibit the issues of information omission, causing the effective length of p deviates significantly from e_i . This results in a lack of crucial information in the extracted features, reflected as insufficient region of interest in the heatmap. Conversely, when θ is too large, as e_j in Figure 4, content features exhibit the issues of information drift, with p being located in the wrong quadrant and its effective direction opposing e_i . This introduces a large amount of incorrect information, reflected as incorrect region of interest in the heatmap.

In such circumstances, the recommendation system is easily to make incorrect recommendations, because the feature representation contradicts the users' preferences, failing to appropriately reflect the characteristics of items or users. In the recommendation task, we aim for a smaller deviation between e'_i and e_i . To formalize this objective, we define an error function $f(e'_i, e_i)$ to measure the gap between the representations:

$$f(e'_i, e_i) = \left(1 - \frac{e'_i \cdot e_i}{\|e'_i\| \|e_i\|} \right) \quad (6)$$

We seek to minimize the expected deviation measure Δ . We can define Δ as:

$$\Delta = \mathbb{E}_{P(e'_i)} [f(e'_i, e_i)] \quad (7)$$

The function $f(e'_i, e_i)$ measures the deviation between representations. In recommendation tasks, the quality of the feature representation e'_i directly affects the accuracy and effectiveness of recommendations. A decline in the quality of e'_i , indicated by an increase in the value of the error function $f(e'_i, e_i)$, denotes an augmented diversity between the representation extracted by the pre-trained encoder e'_i and the ideal representation e_i . Consequently, this leads to an increase in the expected deviation Δ , subsequently influencing the posterior distribution $P(r_{ui}|e_u, e_i)$. Such circumstances may impair the recommendation system's ability to accurately capturing the users' preferences, thereby reducing the accuracy and efficacy of recommendations. By minimizing Δ , we can ensure that the representation e'_i are closer to the ideal representation e_i in expectation. This adaptation of content features enhances the consistency with the ideal representation and thus improves the performance of the recommender system.

4 FEATURE ADAPTER

To address the discovered issues, we proposed Behavior-driven Feature Adapter (BeFA). This is a adapter for adapting multimodal content features that are employed by multimodal recommender systems. Specifically, the content features are first extracted by a pre-trained encoder, and then the content features are adapted by BeFA, and then fed into the multimodal recommender system for item and user modeling. BeFA and the downstream recommender system share the optimization objective and use End-to-End training.

4.1 Problem Formulation

Let $u \in \mathcal{U}$ and $i \in \mathcal{I}$ denote the user and item, respectively. The input behavioral features for user u and item i are represented as $E_{id} \in \mathbb{R}^{d \times (|U|+|I|)}$, where d is the embedding dimension. Each item modality feature is denoted as $E_{i,m} \in \mathbb{R}^{d_m \times |I|}$, where d_m is the dimension of the features, $m \in \mathcal{M}$ represents the modality, and \mathcal{M} is the set of modalities. In this paper, we primarily focus on visual and textual modalities, denoted by $\mathcal{M} = \{v, t\}$. It's worth noting that our approach is adaptable to incorporate more than two modalities.

Next, the users' historical behavior feature is represented as $R \in \{0, 1\}^{|U| \times |I|}$, where each entry $R_{u,i} = 1$ if user u clicked item i , otherwise $R_{u,i} = 0$. This historical interaction data R can naturally be interpreted as a user-item bipartite graph $\mathcal{G} = \{\mathcal{V}, \mathcal{E}\}$. In \mathcal{G} , the vertex set $\mathcal{V} = \mathcal{U} \cup \mathcal{I}$ donates all items and users. The edge set $\mathcal{E} = \{(u, i) | u \in \mathcal{U}, i \in \mathcal{I}, R_{u,i} = 1\}$ represents the interacted users and items. The objective of multimedia recommendation is to accurately predict users' preferences by ranking items for each user based on predicted preference scores $\hat{y}_{u,i}$.

4.2 Behavior-driven Feature Adapter

Due to the shortcomings of pre-trained feature encoders, their extracted content features contain a significant amount of irrelevant and erroneous information. To better utilize modality information, we propose Behaviour-driven Feature Adapter (BeFA) for adapting content features. Firstly, we decouple the original item content features $E_{i,m}$ into features in the decoupled feature space $\hat{E}_{i,m}$:

$$\hat{E}_{i,m} = W_1 E_{i,m} + b_1, \quad (8)$$

where $W_1 \in \mathbb{R}^{d_\lambda \times d_m}$ and $b_1 \in \mathbb{R}^{d_\lambda}$ represent trainable transformation matrix and bias vector, respectively.

Considering that the behavioral information fully reflects the users' preference, we filter the preference-related content features with the help of behavioral information guidance:

$$\ddot{E}_{i,m} = f_{gate}^m(E_{i,id}, \hat{E}_{i,m}) = E_{i,id} \odot \sigma(W_2 \hat{E}_{i,m} + b_2), \quad (9)$$

where $W_2 \in \mathbb{R}^{d_\lambda \times d_\lambda}$ and $b_2 \in \mathbb{R}^{d_\lambda}$ are trainable parameters. Here, \odot denotes element-wise multiplication, and σ is the Tanh non-linear transformation.

Finally, the decoupled content features are recombined. Given that behavioral information reflects user preferences, we determine the weights of different decoupled content features based on the guidance provided by this behavioral information:

$$\bar{E}_{i,m} = f_{merge}^m(E_{i,id}, \ddot{E}_{i,m}) = E_{i,id} \odot \sigma(W_3 \ddot{E}_{i,m} + b_3), \quad (10)$$

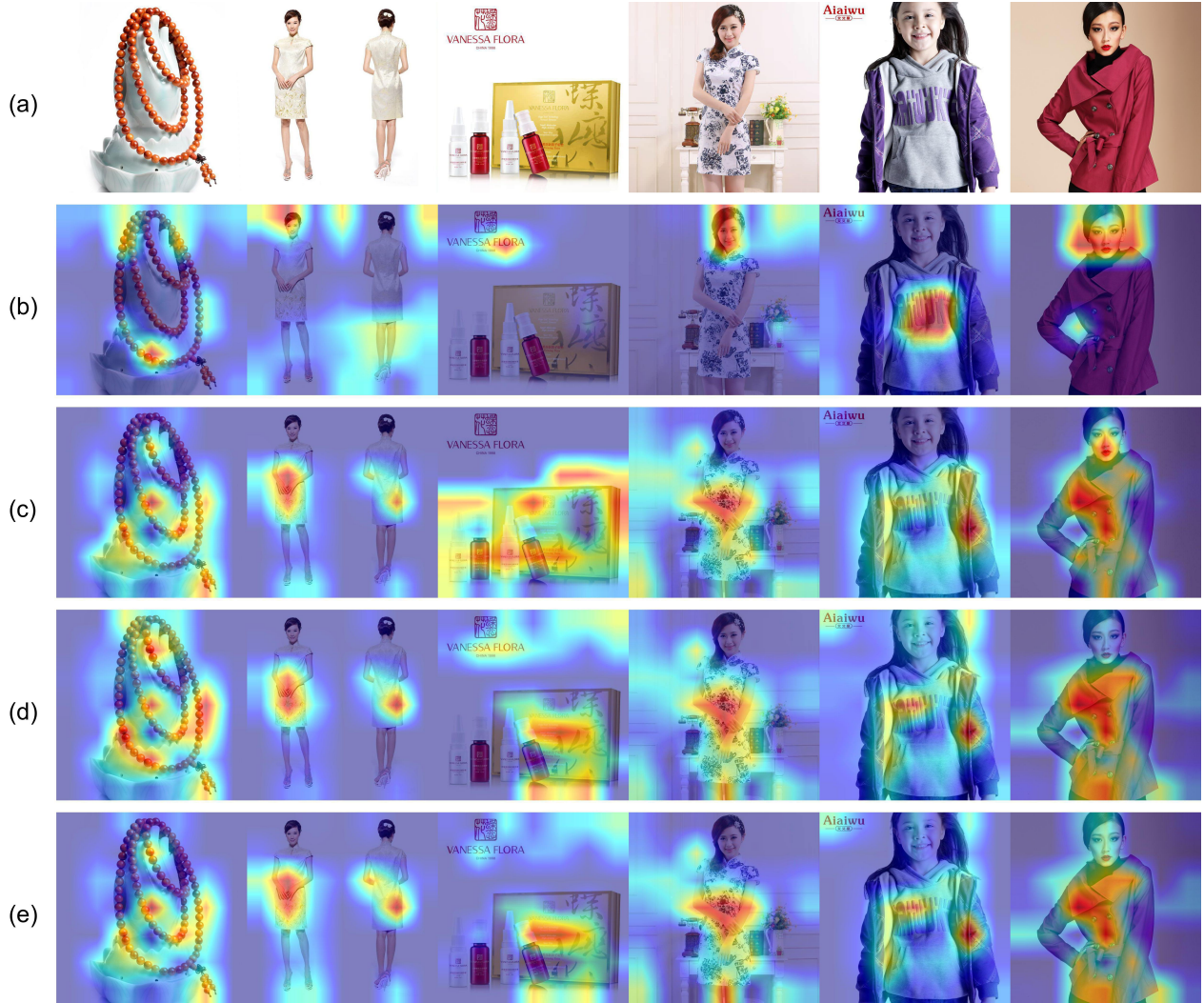


Figure 6: Visual analysis of the effect of adapter on feature purification. (a) is the original image. (b) is the similarity heatmap of the visual features extracted by the pre-trained CLIP. (c) (d) (e) are the similarity heatmaps of the visual features adapted by BeFA applied on FREEDOM, BM3 and LATTICE respectively

where $\mathbf{W}_3 \in \mathbb{R}^{d_\lambda \times d}$ and $\mathbf{b}_3 \in \mathbb{R}^d$ are trainable parameters. Similarly, \odot denotes element-wise multiplication, and σ is the sigmoid non-linear transformation. It is important to note that although Equations 9 and 10 are formally similar, they achieve different effects.

Moreover, we introduce ReLU activation functions and Dropout between each transformation layer. This enables the model to learn non-linear relationships, thereby improving its fitting ability and expressive power. Additionally, it enhances the model’s generalization, making it more suitable for practical application scenarios.

5 EXPERIMENTS

In this section, we conduct extensive experiments to evaluate the performance of the proposed adapter on three public datasets to answer following research questions.

- **RQ1:** How effective is **BeFA** applied to existing multimodal recommender systems?
- **RQ2:** How effective is **BeFA** in adapting content features?
- **RQ3:** Why purifying modality information can achieve better recommendation performance?
- **RQ4:** How do hyper-parameter settings impact the performance of **BeFA**?

5.1 Experimental Settings

5.1.1 Datasets. We conducted experiments on three publicly available datasets: (a) TMALL¹; (b) Microlens²; and (c) H&M³. We performed 10-core filtering on the raw data. The detailed information

¹<https://tianchi.aliyun.com/dataset/140281>

²<https://recsys.westlake.edu.cn/MicroLens-50k-Dataset/>

³<https://www.kaggle.com/datasets/odins0n/handm-dataset-128x128>

Table 2: Performance Comparison on Different Recommender Models. The t-tests validate the significance of performance improvements with p-value ≤ 0.05 .

Encoder	Datasets	TMALL				Microlens				H&M			
		R@10	R@20	N@10	N@20	R@10	R@20	N@10	N@20	R@10	R@20	N@10	N@20
CLIP	BM3	0.0189	0.0298	0.0102	0.0132	0.0510	0.0851	0.0278	0.0375	0.0204	0.0320	0.0114	0.0144
	BM3+BeFA	0.0212	0.0319	0.0115	0.0144	0.0566	0.0911	0.0314	0.0412	0.0266	0.0391	0.0157	0.0190
	<i>Improve</i>	12.17%	7.05%	12.75%	9.09%	10.98%	7.05%	12.95%	9.87%	30.39%	22.19%	37.72%	31.94%
	LATTICE	0.0238	0.0356	0.0134	0.0167	0.0553	0.0886	0.0308	0.0402	0.0289	0.0427	0.0161	0.0197
	LATTICE+BeFA	0.0260	0.0403	0.0183	0.0183	0.0593	0.0943	0.0328	0.0427	0.0317	0.0498	0.0171	0.0217
	<i>Improve</i>	9.24%	13.20%	36.57%	9.58%	7.23%	6.43%	6.49%	6.22%	9.69%	16.63%	6.21%	10.15%
	FREEDOM	0.0212	0.0340	0.0113	0.0148	0.0474	0.0774	0.0262	0.0348	0.0348	0.0526	0.0188	0.0234
	FREEDOM+BeFA	0.0253	0.0375	0.0136	0.0170	0.0503	0.0814	0.0279	0.0368	0.0409	0.0583	0.0226	0.0271
	<i>Improve</i>	19.34%	10.29%	20.35%	14.86%	6.12%	5.17%	6.49%	5.75%	17.53%	10.84%	20.21%	15.81%
	MGCN	0.0249	0.0380	0.0135	0.0171	0.0618	0.0972	0.0342	0.0442	0.0367	0.0549	0.0204	0.0251
	MGCN+BeFA	0.0261	0.0395	0.0142	0.0179	0.0630	0.1000	0.0351	0.0456	0.0405	0.0594	0.0225	0.0274
	<i>Improve</i>	4.82%	3.95%	5.19%	4.68%	1.94%	2.88%	2.63%	3.17%	10.35%	8.20%	10.29%	9.16%
	<i>Avg Improve</i>	11.39%	8.62%	18.71%	9.55%	6.57%	5.38%	7.14%	6.25%	16.99%	14.46%	18.61%	16.77%
	ImageBind	BM3	0.0184	0.0299	0.0097	0.0129	0.0508	0.0842	0.0279	0.0373	0.0195	0.0304	0.0107
BM3+BeFA		0.0224	0.0322	0.0125	0.0152	0.0537	0.0877	0.0299	0.0395	0.0248	0.0378	0.0149	0.0183
<i>Improve</i>		21.74%	7.69%	28.87%	17.83%	5.71%	4.16%	7.17%	5.90%	27.18%	24.34%	39.25%	35.56%
LATTICE		0.0252	0.0374	0.0139	0.0173	0.0580	0.0953	0.0320	0.0426	0.0293	0.0439	0.0164	0.0202
LATTICE+BeFA		0.0266	0.0403	0.0147	0.0184	0.0633	0.1021	0.0340	0.0451	0.0316	0.0498	0.0171	0.0218
<i>Improve</i>		5.56%	7.75%	5.76%	6.36%	9.14%	7.14%	6.25%	5.87%	7.85%	13.44%	4.27%	7.92%
FREEDOM		0.0197	0.0319	0.0107	0.0140	0.0613	0.0976	0.0337	0.0440	0.0364	0.0553	0.0192	0.0241
FREEDOM+BeFA		0.0259	0.0377	0.0141	0.0174	0.0641	0.1004	0.0356	0.0459	0.0417	0.0613	0.0234	0.0285
<i>Improve</i>		31.47%	18.18%	31.78%	24.29%	4.57%	2.87%	5.64%	4.32%	14.56%	10.85%	21.88%	18.26%
MGCN		0.0266	0.0403	0.0144	0.0182	0.0693	0.1075	0.0388	0.0496	0.0405	0.0613	0.0218	0.0272
MGCN+BeFA		0.0275	0.0414	0.0152	0.0185	0.0702	0.1085	0.0389	0.0498	0.0451	0.0655	0.0246	0.0299
<i>Improve</i>		3.38%	2.73%	5.56%	1.65%	1.30%	0.93%	0.26%	0.40%	11.36%	6.85%	12.84%	9.93%
<i>Avg Improve</i>		15.54%	9.09%	17.99%	12.53%	5.18%	3.77%	4.83%	4.12%	15.24%	13.87%	19.56%	17.92%

of the filtered data is presented in Table 1. For multimodal information, we utilized pre-trained CLIP [24] and ImageBind [4] to generate aligned multimodal features.

5.1.2 Comparative Model Evaluation. To verify the prevalence of feature encoder defects, we used ViT-B/32-based CLIP [24] and ImageBind [4] for our experiments. CLIP is a general-purpose feature encoder capable of handling a wide range of data types and application domains. It realizes cross-modality feature representations and exhibits highly efficient performance, making it widely adopted in practical applications and performing well across various tasks. ImageBind is the latest cross-modality feature encoder, which can handle a wider variety of modality information, and achieves a new SOTA performance in the emerging zero-shot recognition task for various modalities, even outperforming the previous specialized models trained specifically for these modalities.

To evaluate the effectiveness of our proposed adapter, we applied it to several representative multimodal recommendation models, including LATTICE [42], BM3 [52], FREEDOM [51], and MGCN [40] for comparison. Additionally, we compared our adapter with existing efficient parameter tuning methods such as LoRA [8] and Soft-Prompt Tuning [13].

i) Multimodal Recommendation Models:

- **LATTICE** [42]: This method designs a new modality-aware structure learning layer that learns the item-item structure of each modality and aggregates multiple modalities to obtain latent item graphs. Based on the learned latent graphs,

graph convolution is performed to explicitly inject higher-order item affinities into item representations.

- **BM3** [52]: This method proposes a simple self-supervised learning framework that generates target views of users or items for comparison learning without negative samples.
- **FREEDOM** [51]: This method devises a degree-sensitive edge pruning method to denoise user-item interaction graphs, rejecting potentially noisy edges with high probability when sampling the graph.
- **MGCN** [40]: This method introduces a behavior-aware fuser to effectively model user preferences by dynamically learning the relative significance of various modality features. Additionally, it integrates the fuser with a self-supervised auxiliary task aimed at maximizing the mutual information between the fused multimodal features and behavioral features. This approach enables the concurrent capture of complementary and supplementary preference information.

ii) Efficient Parameter Tuning Methods

- **Low-Rank Adaptation (LoRA)** [8]: This method aims to enhance the representation of a model while keeping the number of model parameters relatively small. It provides additional learning power by introducing lower rank matrices to linearly transform the hidden representation of the original model. This approach strikes a balance between parameter efficiency and model performance.
- **Soft Prompt Tuning** [13]: This method enhances model performance by fine-tuning small, task-specific embeddings

Table 3: Performance Comparison with other Efficient Parameter Adaptation methods. The best result is in boldface and the second best is underlined. The t-tests validate the significance of performance improvements with p-value ≤ 0.05 .

Dadatasets	TMALL				Microlens				H&M			
	R@10	R@20	N@10	N@20	R@10	R@20	N@10	N@20	R@10	R@20	N@10	N@20
BM3	0.0189	0.0298	0.0102	0.0132	0.0510	0.0851	0.0278	0.0375	<u>0.0204</u>	<u>0.0320</u>	0.0114	<u>0.0144</u>
BM3+LoRA	0.0215	0.0333	0.0117	0.0150	0.0510	0.0850	0.0280	0.0376	0.0191	0.0290	0.0110	0.0135
BM3+SoftPrompt	0.0193	0.0298	0.0102	0.0131	<u>0.0517</u>	<u>0.0861</u>	<u>0.0285</u>	<u>0.0382</u>	0.0202	0.0311	<u>0.0114</u>	0.0142
BM3+BeFA	<u>0.0212</u>	<u>0.0319</u>	<u>0.0115</u>	<u>0.0144</u>	0.0566	0.0911	0.0314	0.0412	0.0266	0.0391	0.0157	0.0190
LATTICE	0.0238	0.0356	0.0134	0.0167	0.0553	0.0886	0.0308	0.0402	0.0289	0.0427	0.0161	0.0197
LATTICE+LoRA	0.0254	0.0384	0.0147	<u>0.0183</u>	0.0550	0.0884	0.0304	0.0399	0.0289	0.0434	0.0163	0.0201
LATTICE+SoftPrompt	0.0266	<u>0.0389</u>	<u>0.0148</u>	0.0182	0.0539	<u>0.0889</u>	0.0294	0.0393	<u>0.0301</u>	<u>0.0459</u>	<u>0.0166</u>	<u>0.0207</u>
LATTICE+BeFA	<u>0.0260</u>	0.0403	0.0183	0.0183	0.0593	0.0943	0.0328	0.0427	0.0317	0.0498	0.0171	0.0217
FREEDOM	0.0212	0.0340	0.0113	0.0148	0.0474	0.0774	0.0262	0.0348	0.0348	0.0526	0.0188	0.0234
FREEDOM+LoRA	0.0197	0.0323	0.0106	0.0141	<u>0.0476</u>	<u>0.0774</u>	<u>0.0264</u>	<u>0.0349</u>	0.0352	0.0533	0.0190	0.0237
FREEDOM+SoftPrompt	0.0215	<u>0.0342</u>	<u>0.0118</u>	<u>0.0154</u>	<u>0.0465</u>	<u>0.0769</u>	<u>0.0258</u>	<u>0.0345</u>	<u>0.0406</u>	<u>0.0577</u>	<u>0.0224</u>	<u>0.0268</u>
FREEDOM+BeFA	0.0243	0.0364	0.0131	0.0164	0.0503	0.0814	0.0279	0.0368	0.0409	0.0583	0.0226	0.0271
MGCN	0.0249	0.0380	0.0135	0.0171	<u>0.0618</u>	<u>0.0972</u>	<u>0.0342</u>	<u>0.0442</u>	0.0367	0.0549	0.0204	0.0251
MGCN+LoRA	0.0260	0.0391	0.0141	0.0179	0.0598	0.0963	0.0335	0.0438	0.0367	0.0554	0.0203	0.0252
MGCN+SoftPrompt	<u>0.0260</u>	<u>0.0391</u>	0.0144	0.0180	0.0597	0.0955	0.0334	0.0435	<u>0.0375</u>	<u>0.0557</u>	<u>0.0207</u>	<u>0.0254</u>
MGCN+BeFA	0.0261	0.0395	<u>0.0142</u>	<u>0.0179</u>	0.0630	0.1000	0.0351	0.0456	0.0405	0.0594	0.0225	0.0274
Avg Improve	2.44%	1.71%	7.89%	0.48%	6.08%	4.98%	6.25%	5.67%	11.11%	9.59%	12.58%	11.44%

(prompts) inserted into the input, thereby adapting pre-trained language models to new tasks without altering their original weights.

5.1.3 Evaluation Protocols. For a fair comparison, we follow the evaluation settings in [42, 52] with the same 8:1:1 data splitting strategy for training, validation and testing. Besides, we follow the all-ranking protocol to evaluate the top-K recommendation performance and report the average metrics for all users in the test set: R@K and N@K, which are abbreviations for Recall@K [23] and NDCG@k [9], respectively.

5.1.4 Implementation Details. We implement MMRec⁴ [50] based on PyTorch, which is a unified public repository designed for multimodal recommendation methods. To ensure fair comparison, we employed the Adam optimizer to optimize all methods and referred to the best hyperparameter settings reported in the original baseline paper. For general settings, we initialized embeddings with Xavier initialization of dimension 64, set the regularization coefficient to $\lambda_E = 10^{-4}$, and batch size to $B = 2048$. Early stopping and total epochs are fixed at 10 and 1000, respectively. We select the best model with the highest Recall@20 metric on the validation set and reported metrics on the test set accordingly.

5.2 Overall performance(RQ1)

5.2.1 Effectiveness.

(a) Comparison of model performance before and after applying BeFA

Table 2 shows the performance comparison of BeFA applied to existing multimodal recommendation models on three datasets. From the table, we find several observations:

- Our adapter significantly improved recommendation performance on all three datasets. Specifically, our adapter

⁴<https://github.com/enoch/MMRec>

has achieved an average improvement of 9.07% and 11.02% over the baseline in terms of Recall@20 and NDCG@20. This suggests that the content features extracted by the pre-trained encoder do have deficiencies that affect recommendation performance. Our processing of content features is very efficient and effectively reduces modality noise. This helps the multimodal recommendation models to better utilize the modality information and thus improve the recommendation performance.

- Our adapter has significant performance improvements for all encoders. All pre-trained feature encoders are generally defective. We use CLIP and ImageBind as an example, and applying our adapter to the multimodal features extracted by these pre-trained feature encoders has led to a significant improvement in the performance of the recommender system. This suggests that the deficiencies are mainly due to the pre-training data, indicating that the content features extracted by the pre-trained encoders generally do not reflect the users' preferences.
- More powerful encoder can extract more sufficient content information. ImageBind has better overall performance than CLIP when applied to recommendation models. This indicates that more advanced encoders are able to extract more sufficient content information. Thus better modelling of users and items to improve the performance of recommendations.

(b) Performance comparison with existing parameter tuning methods

Table 3 shows the comparison between our adapter and existing efficient parameter adaptation methods. From the table, we find several observations:

- The performance of our adapter is overall significantly better than existing efficient parameter tuning methods. This

Table 4: The training cost. #Param: number of tunable parameters, Time/E: averaged training time for one epoch, 's' means seconds. The results are collected on a GeForce RTX 4090 GPU.

Dataset	Method	#Param.	Time/E
TMALL	BM3	9.45M	0.38s
	BM3+LoRA	+4.10K	+0.04s
	BM3+SoftPrompt	+0.13K	+0.02s
	BM3+BeFA	+0.20M	+0.08s
Microlens	BM3	18.36M	0.98s
	BM3+LoRA	+4.10K	+0.07s
	BM3+SoftPrompt	+0.13K	+0.04s
	BM3+BeFA	+0.20M	+0.15s
H&M	BM3	21.26M	1.20s
	BM3+LoRA	+4.10K	+0.04s
	BM3+SoftPrompt	+0.13K	+0.01s
	BM3+BeFA	+0.20M	+0.12s

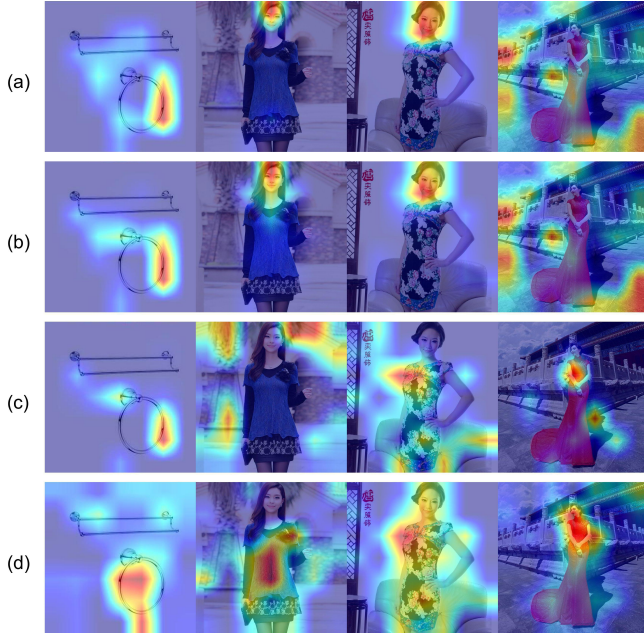


Figure 7: The effect of LoRA and SoftPrompt Turning on the adaptation of features. (a) is the original heatmap, (b) is the heatmap of visual features adapted by LoRA, (c) is the heatmap of visual features adapted by SoftPrompt Turning and (d) is the heatmap of visual features adapted by BeFA.

indicates that our adapter is better suited for the recommendation task than generalized efficient parameter tuning methods. It suggests that our adapter employs behavioral information guidance to more effectively obtain content features related to users' preferences, thereby improving the effectiveness of recommendations.

- Existing parameter tuning approaches are not generalized for recommendation tasks. The performance decreases in

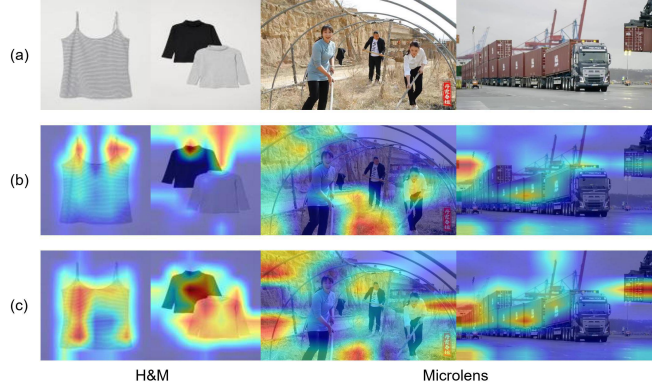


Figure 8: The gaps in the effectiveness of our adapter on different datasets. (a) is the original image. (b) is the heatmap of the visual features extracted by the pre-trained CLIP. (c) is the heatmap of visual features adapted by BeFA.

some cases instead, which indicates that these existing generalized parameter tuning methods are not necessarily suitable for the recommendation tasks. This highlights the importance of incorporating behavioral information guidance in recommendation tasks to improve model performance.

5.2.2 Efficiency. We also analyze the efficiency of our adapter with other existing efficient parameter tuning methods on the BM3 model. The specific model parameter counts and training costs are shown in Table 4. Compared to the overall model training time, our training time increases by only about 15%, indicating that our method is not only effective but also efficient.

Although the design of our adapter is more complex compared to LoRA and Soft-Prompt Turning the increase in the number of parameters after using our adapter is still small compared to the overall parameters of the recommender system itself, ranging from 0.93% to 2.09%. In terms of training costs, the increase in overall training time after using our adapter is still within an acceptable range. The training time for the recommender system using our adapter is comparable to that of using LoRA and Soft-Prompt Turning. This suggests that although our adapter introduces additional parameters, it does not impose a significant burden on the training process. The substantial improvement in performance of our adapter highlights its efficiency, trading a small number of parameters and training time gains for a significant improvement in recommendation accuracy.

5.3 Visualization Analysis(RQ2&RQ3)

5.3.1 Case Study.

(a)Effectiveness with different models

To visually demonstrate the effect of our adapter on content features, we applied it to the proposed visualization attribution analysis. Specifically, before calculating the similarity between content features and behavioral features in the attribution analysis, we processed the content features with our adapter. We then computed similarity weights with the behavioral features and generated new

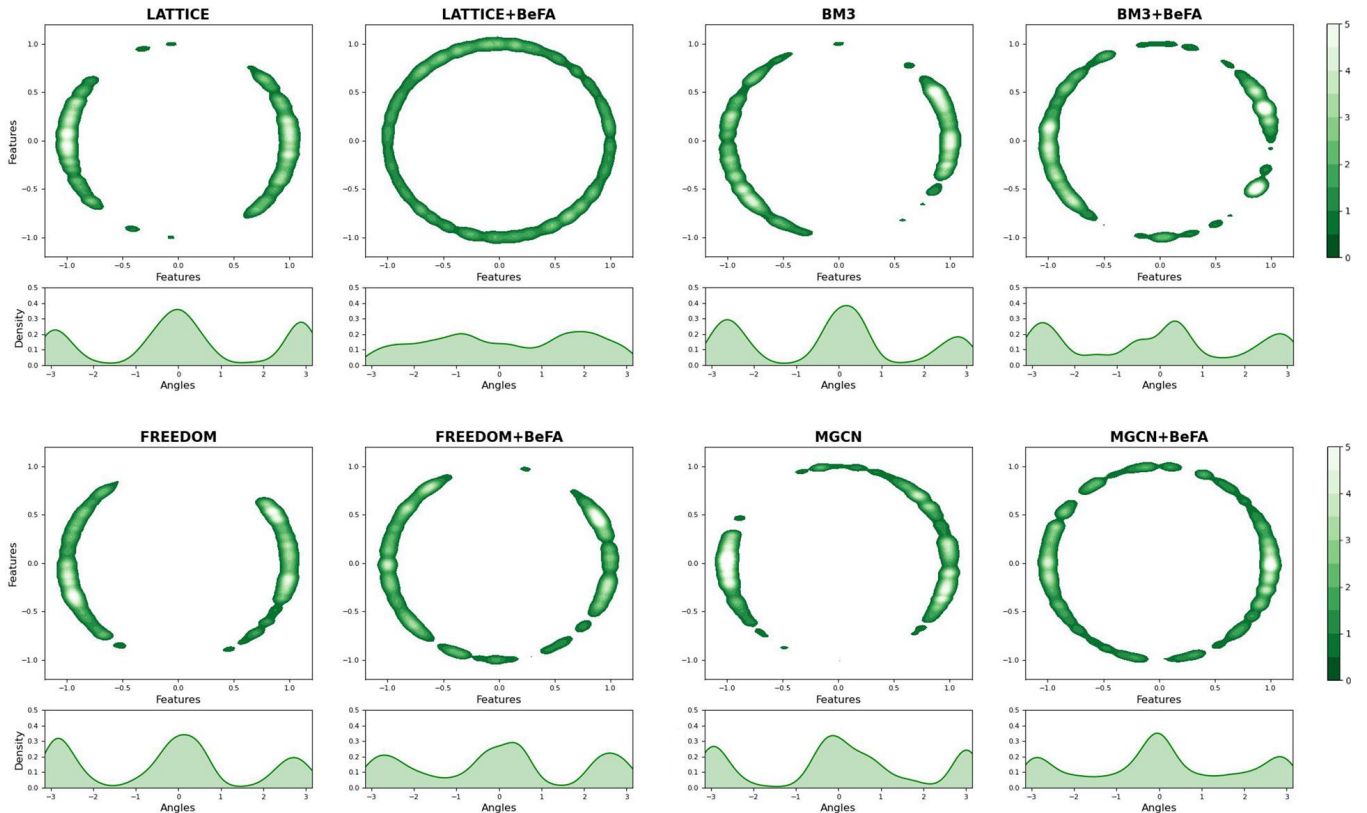


Figure 9: The Distribution of representations in different multimodal recommendation model in visual modalities before and after adaptation by BeFA.

heatmaps using these newly calculated weights with the corresponding masked images.

As shown in Figure 6, by analysing the heatmap before and after our adapter, we can clearly find that our adapter’s enhancement of content features is very obvious. Our adapter significantly improves the attention areas of features extracted by the pre-trained feature encoder, addressing issues of information drift and information omission. The adapted features focus more on the recommended products, with a marked decrease in attention to background elements unrelated to the recommendation. This reduction in noise enhances feature representation and consequently improves recommendation performance.

Additionally, the adapted features more comprehensively capture product details, significantly increasing the coverage of the area of interest for products. This comprehensive extraction of product details not only improves feature recognition but also enhances the recommender system’s ability to model product features. This means that the recommender system is able to more accurately capture the core features of the product, thus providing more relevant and accurate results when making recommendations. Overall, our adapter enables multimodal recommender systems to better utilize content features by using behavioral information to guide feature adaptation, thus significantly improving recommendation performance.

(b) Effectiveness with different encoders

We utilize the content features extracted by two representative multimodal feature encoders, the ViT-32/B version of CLIP and ImageBind, and analyze the heatmaps of the content features within different downstream recommendation models after applying BeFA. Our analysis reveals that the content features extracted by both encoders exhibit issues of information drift and information omission. After applying BeFA, these content features are better focused on the recommended products themselves. This demonstrates that the deficiencies of pre-trained feature encoders are common in multimodal recommendation tasks, while our adapter effectively adapts to the content features extracted by different feature encoders, highlighting its general applicability.

(c) Comparison with existing adaptation methods

We visualize and analyze the content features adapted by LoRA and Soft-Prompt Tuning, as shown in Figure 7. The results indicate that while LoRA and Soft-Prompt Tuning provide some optimization, the degree of adaptation is limited. The adapted content features still exhibit issues such as content error and content insufficiency, failing to focus accurately on the content of the product itself. These methods fail to adequately address the issues of information drift and information omission. This is the reason for the overall poor performance of existing adaptation methods in recommendation tasks. In contrast, the impact of BeFA on content features content

features is significantly better than that of existing methods, which is why BeFA performs well in the recommendation task.

(d) Analysis in different scenarios

We employed three datasets ranging from simple to complex scenarios. The H&M dataset comprises only product images with minimal interference, making it relatively clean. In contrast, the Microlens dataset comprises more complex images with more background interference. Our adapter demonstrated significant improvements across both datasets. Specifically, on the H&M dataset, it increases Recall@20 and NDCG@20 by 14.17% and 17.34%, respectively. Meanwhile, on the Microlens dataset, our adapter increases Recall@20 and NDCG@20 by 4.58% and 5.19%, respectively. These findings indicate the adapter’s effectiveness across varying levels of scene complexity. Moreover, as illustrated in Figure 8, even in complex scenarios, our adapter effectively removes irrelevant information and locates the recommended products as precisely as possible

5.3.2 Representation distribution analysis. To visually demonstrate the impact of BeFA on adjusting content features, we visualize the distribution of visual representations in the TMALL dataset. Figure 9 illustrates the comparison of our adapter’s application to feature distributions across various recommendation models. Specifically, we randomly sample 500 item representations from the TMALL dataset and map them to two-dimensional normalized vectors on the unit hypersphere \mathcal{S}^1 (i.e., a circle with a radius of 1) by using t-SNE [31]. Subsequently, we employ Gaussian kernel density estimation(KDE) [30] to plot the distribution of these two-dimensional features.

Further examining the changes in the distribution of two dimensional features across different recommendation models before and after applying BeFA, we observe that the original feature distribution is more dispersed, forming multiple small dense regions. This distribution indicates that there is a large amount of noise in the visual feature extraction process, hindering the models’ ability to effectively distinguish key features of different products. In contrast, after applying BeFA, the feature distribution becomes more uniform and smooth, which indicates that our adapter has significant effects in eliminating noise. This improvement not only enhances feature recognition capability but also improves the model’s ability to distinguish different content features [32].

Moreover, comparing the changes in feature distributions across different models, it can be found that BeFA has strong adaptability. The feature distributions of various multimodal recommendation models show significant improvements after applying BeFA. This indicates that our adapter is not only effective on a single model but also has strong generalization capabilities across different recommender systems. This adaptability highlights BeFA’s wide potential and value in practical applications.

5.4 Sensitivity Analysis(RQ4)

We investigate the size of the decoupling space relative to the original embedding space, as shown in Fig.10. The results show that the optimal size of the decoupling space is about four times the size of the original embedding space on some datasets. When the decoupling space dimension is small (e.g., 0.125x and 0.25x), it may create an information bottleneck, leading to poor performance across all

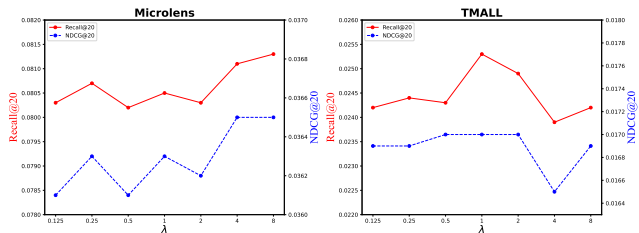


Figure 10: Performance comparison w.r.t. different size of the decoupling space relative to the original embedding space λ .

datasets in both Recall@20 and NCGD@20. A smaller decoupling space cannot hold sufficient information, making it difficult for the model to accurately capture and differentiate features, thereby negatively impacting recommendation performance. Conversely, an excessively large decoupling space dimension may lead to dimensionality catastrophe, introducing noise and redundant features which complicates the model’s ability to effectively distinguish and learn features in a high-dimensional space. Additionally, its number of parameters and the computational cost will increase dramatically, bringing additional burden to the training process, which is impractical for practical application scenarios.

Furthermore, we find that there is a significant difference in the performance of Microlens, TMALL and H&M datasets under varying decoupling space sizes. For the Microlens dataset, both Recall@20 and NCGD@20 achieve the optimal performance when the decoupling space size is four times of the original embedding space. In contrast, in the TMALL dataset, although the overall trend is similar, the optimal point fluctuates slightly, suggesting that the size of the decoupling space may need to be adjusted on different datasets to obtain optimal results. The overall adapter performance fluctuates greatly with the change in the decoupling space size, highlighting the challenge of finding the optimal size. This is one of the limitations of our work, which could be addressed by considering the decoupling space size as a learnable parameter in future research. This approach could adaptively adjust the decoupling space size for different application scenarios to achieve the best performance.

6 CONCLUSION

In this paper, we introduce an attribution analysis for visually analyzing deficiencies of the content features. We found that the content features of certain products suffer from information drift and information omission, and theoretically prove that these deficiencies lead to a decrease in the performance of the recommender systems. To address these issues, we propose Behavior-driven Feature Adapter (BeFA) adapter which adapts content features through the guidance of behavioral information, thereby enhancing the expressiveness of the content features and significantly improve the performance of the recommender systems

In our future work, we consider introducing the size of the decoupling space as a learnable parameter into the training of the adapter, so that the optimized performance can be achieved in different scenarios, enhancing its general applicability.

REFERENCES

- [1] CHEN, L., WU, L., HONG, R., ZHANG, K., AND WANG, M. Revisiting graph based collaborative filtering: A linear residual graph convolutional network approach. In *Proceedings of the AAAI conference on artificial intelligence* (2020), vol. 34, pp. 27–34.
- [2] CHEN, P., LI, Q., BIAZ, S., BUI, T., AND NGUYEN, A. gscorecam: What objects is clip looking at? In *Proceedings of the Asian Conference on Computer Vision* (2022), pp. 1959–1975.
- [3] DOSOVITSKIY, A., BEYER, L., KOLESNIKOV, A., WEISSENORN, D., ZHAI, X., UNTERTHINER, T., DEGHANI, M., MINDERER, M., HEIGOLD, G., GELLY, S., ET AL. An image is worth 16x16 words: Transformers for image recognition at scale. *arXiv preprint arXiv:2010.11929* (2020).
- [4] GIRDHAR, R., EL-NOUBY, A., LIU, Z., SINGH, M., ALWALA, K. V., JOULIN, A., AND MISRA, I. Imagebind: One embedding space to bind them all. In *Proceedings of the IEEE/CVF Conference on Computer Vision and Pattern Recognition* (2023), pp. 15180–15190.
- [5] HE, K., ZHANG, X., REN, S., AND SUN, J. Deep residual learning for image recognition. In *Proceedings of the IEEE conference on computer vision and pattern recognition* (2016), pp. 770–778.
- [6] HE, R., AND MCAULEY, J. Vbpr: visual bayesian personalized ranking from implicit feedback. In *Proceedings of the AAAI conference on artificial intelligence* (2016), vol. 30.
- [7] HOWARD, J., AND RUDER, S. Universal language model fine-tuning for text classification. *arXiv preprint arXiv:1801.06146* (2018).
- [8] HU, E. J., SHEN, Y., WALLIS, P., ALLEN-ZHU, Z., LI, Y., WANG, S., WANG, L., AND CHEN, W. Lora: Low-rank adaptation of large language models. *arXiv preprint arXiv:2106.09685* (2021).
- [9] JÄRVELIN, K., AND KEKÄLÄINEN, J. Cumulated gain-based evaluation of ir techniques. *ACM Transactions on Information Systems (TOIS)* 20, 4 (2002), 422–446.
- [10] JIN, Y., LI, Y., YUAN, Z., AND MU, Y. Learning instance-level representation for large-scale multi-modal pretraining in e-commerce. In *Proceedings of the IEEE/CVF Conference on Computer Vision and Pattern Recognition* (2023), pp. 11060–11069.
- [11] JU, H., KANG, S., LEE, D., HWANG, J., JANG, S., AND YU, H. Multi-domain recommendation to attract users via domain preference modeling. In *Proceedings of the AAAI Conference on Artificial Intelligence* (2024), vol. 38, pp. 8582–8590.
- [12] KHURANA, D., KOLI, A., KHATTER, K., AND SINGH, S. Natural language processing: State of the art, current trends and challenges. *Multimedia tools and applications* 82, 3 (2023), 3713–3744.
- [13] LESTER, B., AL-ROUF, R., AND CONSTANT, N. The power of scale for parameter-efficient prompt tuning. *arXiv preprint arXiv:2104.08691* (2021).
- [14] LI, B., LI, F., GAO, S., FAN, Q., LU, Y., HU, R., AND ZHAO, Z. Efficient prompt tuning for vision and language models. In *International Conference on Neural Information Processing* (2023), Springer, pp. 77–89.
- [15] LI, H., SUN, J., XU, Z., AND CHEN, L. Multimodal 2d+ 3d facial expression recognition with deep fusion convolutional neural network. *IEEE Transactions on Multimedia* 19, 12 (2017), 2816–2831.
- [16] LIU, J., SUN, L., NIE, W., JING, P., AND SU, Y. Graph disentangled contrastive learning with personalized transfer for cross-domain recommendation. In *Proceedings of the AAAI Conference on Artificial Intelligence* (2024), vol. 38, pp. 8769–8777.
- [17] LIU, Y., PHAM, T.-A. N., CONG, G., AND YUAN, Q. An experimental evaluation of point-of-interest recommendation in location-based social networks. *Proc. VLDB Endow.* 10 (2017), 1010–1021.
- [18] LU, W., CHEN, S., LI, K., AND LAKSHMANAN, L. V. Show me the money: Dynamic recommendations for revenue maximization. *Proceedings of the VLDB Endowment* 7, 14 (2014), 1785–1796.
- [19] MACHANAVAJJHALA, A., KOROLOVA, A., AND SARMA, A. D. Personalized social recommendations—accurate or private? *arXiv preprint arXiv:1105.4254* (2011).
- [20] NI, Y., CHENG, Y., LIU, X., FU, J., LI, Y., HE, X., ZHANG, Y., AND YUAN, F. A content-driven micro-video recommendation dataset at scale. *arXiv preprint arXiv:2309.15379* (2023).
- [21] PAPANAKIS, H., PAPANIGORIOU, A., PANAGIOTAKIS, C., KOSMAS, E., AND FRAGOPOULOU, P. Collaborative filtering recommender systems taxonomy. *Knowledge and Information Systems* 64, 1 (2022), 35–74.
- [22] PARCHAS, P., NAAMAD, Y., VAN BOUWEL, P., FALOUTSOS, C., AND PETROPOULOS, M. Fast and effective distribution-key recommendation for amazon redshift. *Proceedings of the VLDB Endowment* 13, 12 (2020), 2411–2423.
- [23] POWERS, D. M. Evaluation: from precision, recall and f-measure to roc, informedness, markedness and correlation. *arXiv preprint arXiv:2010.16061* (2020).
- [24] RADFORD, A., KIM, J. W., HALLACY, C., RAMESH, A., GOH, G., AGARWAL, S., SASTRY, G., ASKELL, A., MISHKIN, P., CLARK, J., ET AL. Learning transferable visual models from natural language supervision. In *International conference on machine learning* (2021), PMLR, pp. 8748–8763.
- [25] RANZATO, M., SUSSKIND, J., MNH, V., AND HINTON, G. On deep generative models with applications to recognition. In *CVPR 2011* (2011), IEEE, pp. 2857–2864.
- [26] RINALDI, A. M., RUSSO, C., AND TOMMASINO, C. Automatic image captioning combining natural language processing and deep neural networks. *Results in Engineering* 18 (2023), 101107.
- [27] SELVARAJU, R. R., COGSWELL, M., DAS, A., VEDANTAM, R., PARIKH, D., AND BATRA, D. Grad-cam: Visual explanations from deep networks via gradient-based localization. In *Proceedings of the IEEE international conference on computer vision* (2017), pp. 618–626.
- [28] SUN, X., HU, P., AND SAENKO, K. Dualcoop: Fast adaptation to multi-label recognition with limited annotations. *Advances in Neural Information Processing Systems* 35 (2022), 30569–30582.
- [29] TAO, Z., LIU, X., XIA, Y., WANG, X., YANG, L., HUANG, X., AND CHUA, T.-S. Self-supervised learning for multimedia recommendation. *IEEE Transactions on Multimedia* 25 (2023), 5107–5116.
- [30] TERRELL, G. R., AND SCOTT, D. W. Variable kernel density estimation. *The Annals of Statistics* (1992), 1236–1265.
- [31] VAN DER MAATEN, L., AND HINTON, G. Visualizing data using t-sne. *Journal of machine learning research* 9, 11 (2008).
- [32] WANG, C., YU, Y., MA, W., ZHANG, M., CHEN, C., LIU, Y., AND MA, S. Towards representation alignment and uniformity in collaborative filtering. In *Proceedings of the 28th ACM SIGKDD conference on knowledge discovery and data mining* (2022), pp. 1816–1825.
- [33] WANG, H., WANG, Z., DU, M., YANG, F., ZHANG, Z., DING, S., MARDZIEL, P., AND HU, X. Score-cam: Score-weighted visual explanations for convolutional neural networks. In *Proceedings of the IEEE/CVF conference on computer vision and pattern recognition workshops* (2020), pp. 24–25.
- [34] WANG, Q., WEI, Y., YIN, J., WU, J., SONG, X., AND NIE, L. Dualgnn: Dual graph neural network for multimedia recommendation. *IEEE Transactions on Multimedia* 25 (2021), 1074–1084.
- [35] WEI, W., TANG, J., JIANG, Y., XIA, L., AND HUANG, C. Promptmm: Multi-modal knowledge distillation for recommendation with prompt-tuning. *arXiv preprint arXiv:2402.17188* (2024).
- [36] WEI, Y., WANG, X., NIE, L., HE, X., AND CHUA, T.-S. Graph-refined convolutional network for multimedia recommendation with implicit feedback. In *Proceedings of the 28th ACM international conference on multimedia* (2020), pp. 3541–3549.
- [37] WEI, Y., WANG, X., NIE, L., HE, X., HONG, R., AND CHUA, T.-S. Mimgcn: Multi-modal graph convolution network for personalized recommendation of micro-video. In *Proceedings of the 27th ACM international conference on multimedia* (2019), pp. 1437–1445.
- [38] WU, S., SUN, F., ZHANG, W., XIE, X., AND CUI, B. Graph neural networks in recommender systems: a survey. *ACM Computing Surveys* 55, 5 (2022), 1–37.
- [39] YU, J., YIN, H., XIA, X., CHEN, T., CUI, L., AND NGUYEN, Q. V. H. Are graph augmentations necessary? simple graph contrastive learning for recommendation. In *Proceedings of the 45th international ACM SIGIR conference on research and development in information retrieval* (2022), pp. 1294–1303.
- [40] YU, P., TAN, Z., LU, G., AND BAO, B.-K. Multi-view graph convolutional network for multimedia recommendation. In *Proceedings of the 31st ACM International Conference on Multimedia* (2023), pp. 6576–6585.
- [41] YUAN, Z., YUAN, F., SONG, Y., LI, Y., FU, J., YANG, F., PAN, Y., AND NI, Y. Where to go next for recommender systems? id-vs. modality-based recommender models revisited. In *Proceedings of the 46th International ACM SIGIR Conference on Research and Development in Information Retrieval* (2023), pp. 2639–2649.
- [42] ZHANG, J., ZHU, Y., LIU, Q., WU, S., WANG, S., AND WANG, L. Mining latent structures for multimedia recommendation. In *Proceedings of the 29th ACM international conference on multimedia* (2021), pp. 3872–3880.
- [43] ZHANG, J., ZHU, Y., LIU, Q., ZHANG, M., WU, S., AND WANG, L. Latent structure mining with contrastive modality fusion for multimedia recommendation. *IEEE Transactions on Knowledge and Data Engineering* (2022).
- [44] ZHANG, R., LIU, Q.-D., WEI, J.-X., ET AL. Collaborative filtering for recommender systems. In *2014 second international conference on advanced cloud and big data* (2014), IEEE, pp. 301–308.
- [45] ZHANG, W., ZHANG, Y., MA, L., GUAN, J., AND GONG, S. Multimodal learning for facial expression recognition. *Pattern Recognition* 48, 10 (2015), 3191–3202.
- [46] ZHOU, B., KHOSLA, A., LAPEDRIZA, A., OLIVA, A., AND TORRALBA, A. Learning deep features for discriminative localization. In *Proceedings of the IEEE conference on computer vision and pattern recognition* (2016), pp. 2921–2929.
- [47] ZHOU, H., ZHOU, X., ZENG, Z., ZHANG, L., AND SHEN, Z. A comprehensive survey on multimodal recommender systems: Taxonomy, evaluation, and future directions. *arXiv preprint arXiv:2302.04473* (2023).
- [48] ZHOU, H., ZHOU, X., ZHANG, L., AND SHEN, Z. Enhancing dyadic relations with homogeneous graphs for multimodal recommendation. In *ECAI 2023*. IOS Press, 2023, pp. 3123–3130.
- [49] ZHOU, K., YANG, J., LOY, C. C., AND LIU, Z. Conditional prompt learning for vision-language models. In *Proceedings of the IEEE/CVF conference on computer vision and pattern recognition* (2022), pp. 16816–16825.
- [50] ZHOU, X. Mmrec: Simplifying multimodal recommendation. In *Proceedings of the 5th ACM International Conference on Multimedia in Asia Workshops* (2023), pp. 1–2.
- [51] ZHOU, X., AND SHEN, Z. A tale of two graphs: Freezing and denoising graph structures for multimodal recommendation. In *Proceedings of the 31st ACM International Conference on Multimedia* (2023), pp. 935–943.
- [52] ZHOU, X., ZHOU, H., LIU, Y., ZENG, Z., MIAO, C., WANG, P., YOU, Y., AND JIANG, F.

Bootstrap latent representations for multi-modal recommendation. In *Proceedings of the ACM Web Conference 2023* (2023), pp. 845–854.

[53] ZHU, B., NIU, Y., HAN, Y., WU, Y., AND ZHANG, H. Prompt-aligned gradient

for prompt tuning. In *Proceedings of the IEEE/CVF International Conference on Computer Vision* (2023), pp. 15659–15669.